Nonlinear optical spectroscopy of photonic metamaterials

Evgenia Kim,[1] Feng Wang,[1] Wei Wu,[2] Zhaoning Yu,[2] and Y. Ron Shen[1]
[1]*Department of Physics, University of California, Berkeley, California 94720, USA*
[2]*Quantum Science Research, HP Labs, Hewlett-Packard, Palo Alto, California 94304, USA*
(Received 8 July 2008; published 10 September 2008)

We have obtained spectra of second-harmonic generation, third-harmonic generation, and four-wave mixing from a fishnet metamaterial around its magnetic resonance. The resonant behaviors are distinctly different from those for ordinary materials. They result from the fact that the resonance is plasmonic, and its enhancement appears through the local field in the nanostructure.

DOI: 10.1103/PhysRevB.78.113102 PACS number(s): 78.20.Ci, 42.65.Ky, 42.70.Qs, 78.67.−n

Optical metamaterials with nanoscale metal building blocks have been studied extensively in recent years.[1–8] With each metal unit much smaller than optical wavelength, they can be viewed as continuous media and the metal units act as "artificial molecules." The optical properties of metamaterials can be engineered by proper design of the artificial molecules to exhibit unusual behavior that is nonexistent in nature, such as negative refractive indices. While linear optical properties of metamaterials have been well investigated,[1–8] nonlinear optical properties began to attract interest only recently.[9–15] Such interest stems from possible strong enhancement of nonlinear response from plasmon resonances of the metal nanostructures together with spectral tunability offered by design of artificial molecules.

The experimental nonlinear optical studies of metamaterials reported so far are limited to harmonic generation from nanostructures using a fixed excitation wavelength.[9,10] Enhancement at the magnetic resonance was inferred from comparison of signals from metamaterial structures of different dimensions with corresponding shifted resonant frequencies. Although the approach is informative, it has intrinsic limitations: even in the ideal case of perfectly fabricated metamaterial structures that differ only in scaled size, they can have different local-field distributions in excitation, which can strongly influence the nonlinear output. Separating contributions from local-field distribution and resonance enhancement in the output is difficult. As a result, interpretation of the observed magnetic-resonance enhancement in harmonic generation from a metamaterial is still being debated. For better understanding of resonant nonlinear optical properties of a metamaterial, we realize that it is essential to perform true nonlinear spectroscopy measurement on metamaterials with tunable light source.

In this Brief Report, we present spectroscopic study of second-harmonic generation (SHG), third-harmonic generation (THG), and four-wave mixing from a metamaterial comprising a monolayer of "fishnet" structure.[16,17] It was designed to have negative refractive index at the near-IR range with a magnetic resonance around 1.55 μm.[18] The spectra of SHG and THG with the fundamental input scanned over the magnetic resonance were obtained with different fundamental and harmonic polarizations. Resonant enhancements were clearly observed. Interestingly, the observed resonances are much sharper than that in linear absorption. This is distinctly different from typical molecular cases where resonant excitation at the fundamental wavelength yields the same resonance spectrum in linear and nonlinear responses. Such difference originates from the fact that, unlike molecular resonances, the resonances in metal nanostructures are collective oscillations and their resonance enhancement appears through the local-field effect in the nonlinear process.

The measurements were carried out on a metamaterial sample composed of two silver sheets with hole arrays separated by a silica layer, known as fishnet structure. It was fabricated on a 0.5-mm-thick silica substrate using combination of nanoimprint lithography (NIL) and electron-beam lithography (EBL).[19] The overall area of the fishnet structure was 500×500 μm^2. The scanning electron microscopy (SEM) image of the structure is shown in Fig. 1(a), and the structural configuration and dimensions in Fig. 1(b). Linear optical response of this metamaterial exhibits a magnetic resonance at ~1.55 μm when the magnetic-field component of the input wave threads the loop formed by linking the broad metal wires of the two layers, as indicated in Fig. 1(b) by the black arrows.[18] The measured linear transmittance and

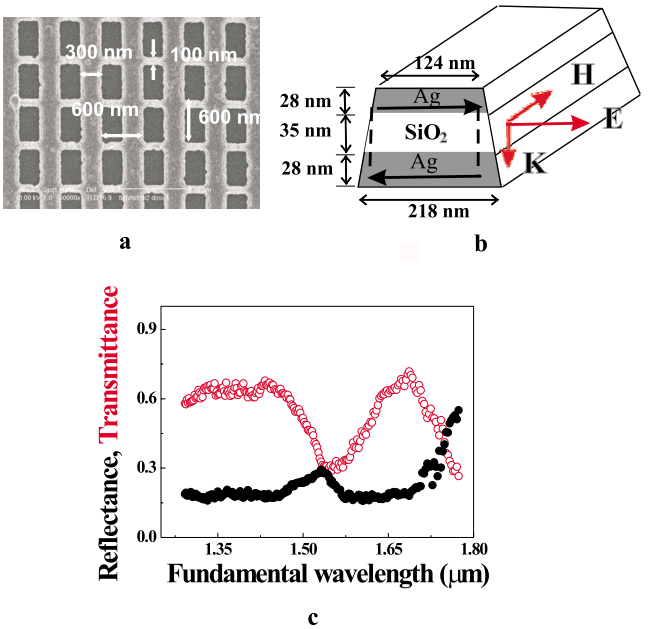

FIG. 1. (Color online) (a) SEM image of the fishnet structure; (b) Schematic cross section of the broad wire of fishnet $Ag/SiO_2/Ag$ structure. (c) Linear transmittance (open dots) and reflectance (solid dots) spectra.

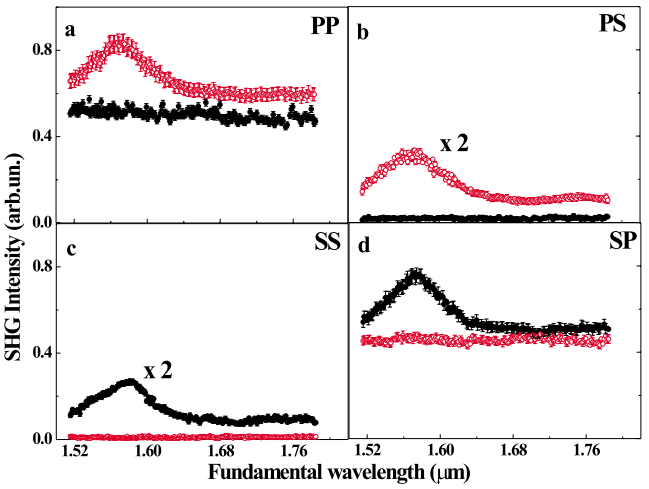

FIG. 2. (Color online) SHG spectra of the fishnet structure for different polarization combinations: (a) *P* in *P* out, (b) *P* in *S* out, (c) *S* in *S* out, and (d) *S* in *P* out. Solid and open dots are for beam geometry with the incident magnetic-field component along and perpendicular to the broad Ag wire, respectively.

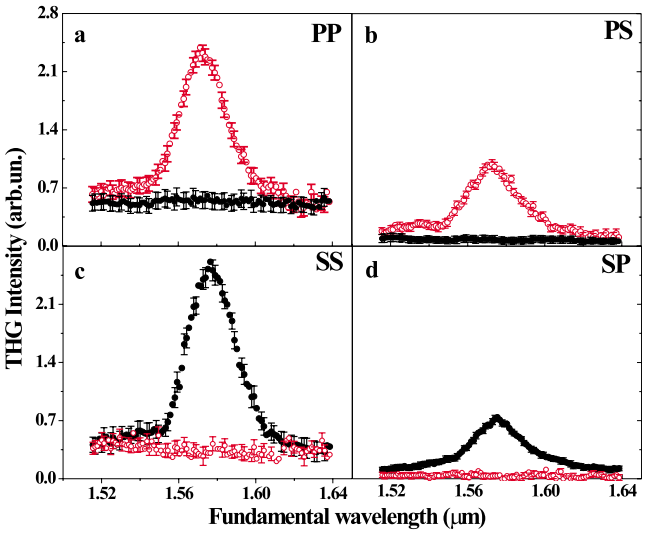

FIG. 3. (Color online) THG spectra of the fishnet structure for different polarization combinations: (a) *P* in *P* out, (b) *P* in *S* out, (c) *S* in *S* out, and (d) *S* in *P* out. Solid and open dots are for beam geometry with the incident magnetic-field component along and perpendicular to the broad Ag wire, respectively.

reflectance spectra are presented in Fig. 1(c). From the amplitude and phase of the linear response, it can be shown that the structure exhibits a negative index of refraction in the wavelength range of 1.45–1.6 μm. (See Ref. 18 for detail.)

The nonlinear optical spectroscopy of the fishnet structure was performed using the tunable output from an optical parametric system, pumped by the third harmonic of a picosecond neodymium-doped yttrium aluminum garnet (Nd:YAG) laser. It generated widely tunable IR pulses at 20 Hz with ~ 7 cm^{-1} spectral width and 20 ps pulse duration. The tunable IR beam(s) was incident at 30° on the sample and focused on a spot of ~ 400 μm with a fluence of about 320 μJ/cm^2. The reflected SHG, THG, and four-wave mixing signal were detected by a photomultiplier, and gated electronics system after polarization selection and spectral filtering.

The SHG spectra, obtained with the incident plane along (solid dots) and perpendicular (open dots) to the broad Ag wires of the fishnet are shown in Fig. 2. Polarization combinations employed are indicated in the figure (*PS*, for example, denotes *P* and *S* polarizations for the fundamental input and SH output, respectively). To correct for the wavelength dependent incident laser intensity, the SHG signals at each wavelength were normalized to that of a smooth silver film with the *PP* polarization combination. Two features are clear in the SHG spectra. First, the SHG spectra display a resonance at 1.55 μm whenever the input polarization has a magnetic-field component along the broad wires of the fishnet (i.e., *P* or *S* polarized when the incident plane is perpendicular to or along the broad wires, respectively) so that the magnetic resonance can be excited. Otherwise, the SHG spectra are featureless with only nonresonant contribution. Second, the *PS* and *SS* polarizations yield weaker SHG signals with a much lower nonresonant background compared to *PP* and *SP*. Presumably this is the result of symmetry. As in the case of thin Ag films, SHG from a perfect fishnet structure, with the incident plane coinciding with a mirror plane, is strictly forbidden for *PS* and *SS* polarizations but allowed for *PP* and *SP*. That SHG with *SS* and *PS* is actually observable is an indication that the fishnet sample is not ideally symmetric.

In Fig. 3, the THG spectra are shown for different sample orientations and polarization combinations using the same notations as those for SHG in Fig. 2. Strong enhancement of THG is observed when and only when the magnetic resonance is excited by the fundamental beam. The stronger signal for *PP* and *SS* compared with *PS* and *SP* polarization can also be understood from symmetry argument: THG with *PS* and *SP* is forbidden in a perfect fishnet structure when the incident plane coincides with a mirror plane. Compared with the SHG spectra, the nonresonant contribution is smaller in the THG signal and the resonance is more pronounced.

We compare in Fig. 4 the magnetic resonant features in the *PP* spectra of linear absorption, SHG, and THG. The resonance of THG is clearly narrower than that of SHG, which is in turn sharper than that of linear absorption. This is in striking contrast with resonance behavior of natural molecular materials. For a molecular material, the nonlinear susceptibility for SHG or THG with input frequency near a resonance, $\omega \sim \omega_R$, is proportional to $1/(\omega \sim \omega_R + i\Gamma_R)$, with Γ_R denoting a phenomenological damping constant.[20] Therefore the resonance in the nonlinear optical processes is characterized by the same resonance as in the linear optical response. The sharper resonances of SHG and THG observed in metamaterials indicate that they are characteristically different from those of ordinary molecular media. The difference arises because plasmon resonances of metal nanostructures are intrinsically collective in nature instead of local as in molecular transitions. Such distinctions do not show up in linear optical properties but become obvious in nonlinear optical spectra where a resonant input field participates multiple times in the nonlinear process.

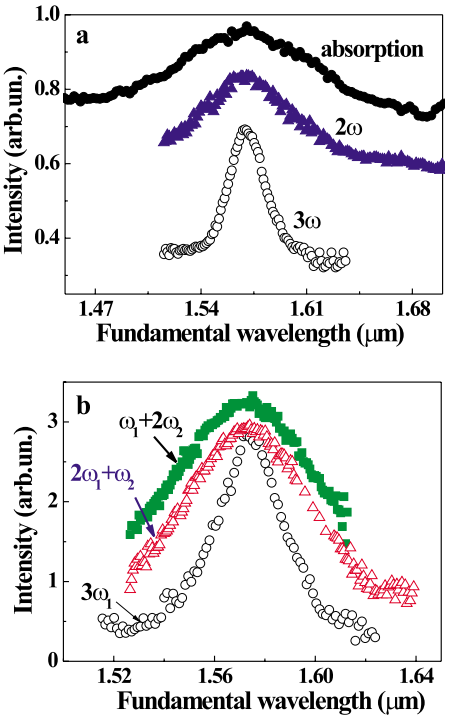

FIG. 4. (Color online) (a) Comparison of SHG (triangle) and THG (open dots) spectra in *PP* polarization combinations with the linear absorption spectrum (solid dots). (b) Spectra of four-wave processes at $3\omega_1$ (open dots), $2\omega_1+\omega_2$ (open triangles), and $\omega_1+2\omega_2$ (squares). The signal strengths at $2\omega_1+\omega_2$ and $\omega_1+2\omega_2$ are scaled up by 6.6 and 43, respectively, for ease of comparison.

To further establish the above-mentioned characteristic resonant behavior in nonlinear responses of metamaterials, we measured outputs of four-wave mixing at $3\omega_1$, $2\omega_1+\omega_2$, and $\omega_1+2\omega_2$, with ω_2 fixed (at wavelength of 1064 nm) and ω_1 scanned across the magnetic resonance. The observed spectra with *PP* polarization are displayed in Fig. 4(b) with signals at $2\omega_1+\omega_2$ and $\omega_1+2\omega_2$ scaled by 6.6 and 43, respectively. It is obvious that each additional ω_1 component in the input leads to extra enhancement of the output at resonance, and the corresponding resonance peak becomes increasingly sharper.

For better understanding of the observed results, we realize that the real source of nth harmonic generation in metamaterials is the induced effective electric dipole on each nanostructural unit,

$$\vec{p}^{(n)} = \int_V \overleftrightarrow{L}(\vec{r},n\omega):\overleftrightarrow{\chi}^{(n)}(\vec{r}):[\vec{E}_{\rm loc}(\vec{r},\omega)]^n dV, \qquad (1)$$

where the integration is over the volume of the unit, $\overleftrightarrow{\chi}^{(n)}$ is the local nth-order nonlinear susceptibility, and $\vec{E}_{\rm loc}(\vec{r},\omega) = \overleftrightarrow{L}(\vec{r},\omega):\vec{E}_0(\omega)$ is the local field, with $\overleftrightarrow{L}(\vec{r},\omega)$ being the local-field correction factor and $\vec{E}_0(\omega)$ the input field. For simplicity, we have neglected the contribution of magnetic dipole and electric quadrupole on $\vec{p}^{(n)}$ in Eq. (1) at the harmonic wavelength. The harmonic output with polarization along $\hat{n}$ is given by $S^{(n)} \propto |\hat{n}\cdot\vec{p}^{(n)}|^2$. Resonances in the response of metamaterials appear through the local field, which can be decomposed into two components: one associated with the magnetic resonance and the other nonresonant. The resonant component is relatively enhanced when ω approaches a plasmon resonance. Thus we can write the local-field correction factor as $\overleftrightarrow{L}(\vec{r},\omega)=\overleftrightarrow{A}(\vec{r},\omega)+\overleftrightarrow{B}(\vec{r},\omega)/D(\omega)$ with D approximated by $D=\omega-\omega_0+i\Gamma$, here describing the magnetic plasmon resonance.

The symmetry requirement for harmonic generation is naturally incorporated in the volume integration of Eq. (1), which, for example, vanishes for symmetry-forbidden processes in a perfect fishnet structure. The integral depends sensitively on the field distribution, and nonresonant and resonant terms can be affected differently because they have different spatial dependences: for a symmetry-forbidden harmonic generation process, if symmetry-breaking modification of the nanostructure is not severe, the nonresonant signal is still expected to be small. At resonance, however, $\overleftrightarrow{B}(\vec{r},\omega)$ is different from $\overleftrightarrow{A}(\vec{r},\omega)$, and can have a spatial distribution emphasizing contribution from the symmetry-breaking part of the structure,[21] generating a relatively strong resonant harmonic output. This explains our observation of resonant spectra with very weak nonresonant background for symmetry-forbidden harmonic generation processes in the fishnet structure presented in Figs. 2 and 3. Numerical calculation on a realistic fishnet structure hopefully will quantify the different effects of symmetry breaking on resonant and nonresonant harmonic generations.

If the nonresonant part of $\overleftrightarrow{L}_{\rm loc}$ could be neglected, we would have, for the nth harmonic generation, $\vec{p}^{(n)} \propto |D|^{-n}$ and $S^{(n)} \propto |D|^{-2n}$. With the presence of the nonresonant $\overleftrightarrow{A}(\vec{r},\omega)$ term in $\overleftrightarrow{L}(\vec{r},\omega)$, the signal $S^{(n)}$ now has terms of $|D|^{-2m}$ with $m=0,1,..n$, and its resonant line shape often appears broader than $|D|^{-2n}$. However, the $|D|^{-2n}$ term is always significant, making the THG ($n=3$) spectrum sharper than SHG ($n=2$), and similarly in comparing spectra of wave mixing at $3\omega_1$, $2\omega_1+\omega_2$, and $\omega_1+2\omega_2$. We note that although local-field effects are well known in plasmonic optical response, its contribution in metamaterial nonlinear response and the consequent sharpening of the nonlinear resonances have never been predicted before.

We can understand sharpening of resonances in the above nonlinear optical effects more physically: plasmons in a metamaterials can be regarded as polaritons. Incoming waves near the plasmon frequency are converted into plasmon-polariton waves in the medium. They then interact in the medium to generate the nonlinear output. The resonance effect comes in the excitation of plasmon polaritons, and therefore exhibits the multiresonant behavior when a nonlinear optical process involves several input waves with frequencies near the same resonance.

In summary, we have measured spectra of SHG, THG, and four-wave mixing from a fishnet metamaterial around its magnetic resonance with different input/output polarization combinations. The results show that the resonant enhancement is much stronger in nonlinear optical response than that in the linear case, and the more times the resonant input field participates in the mixing process, the sharper the resonant

spectrum appears to be. This is because the resonance is plasmonic in nature and shows up in the local-field correction factors in the nonlinear responses. Such resonant behavior is expected to appear in all nonlinear optical processes involving plasmon resonances in metamaterials. This fundamental difference in nonlinear optical behaviors of metamaterials and natural materials should be important in design consideration of nonlinear optical metamaterial based on analogy to ordinary nonlinear optical materials.

E.K., F.W., and Y.R.S. were supported by the Director, Office of Science, Office of Basic Energy Sciences, Materials Sciences and Engineering Division, of the U.S. Department of Energy under Contract No. DE-AC03-76SF00098.

[1] J. B. Pendry, Phys. Rev. Lett. **85**, 3966 (2000).
[2] R. A. Shelby, D. R. Smith, and S. Schultz, Science **292**, 77 (2001).
[3] T. J. Yen, W. J. Padilla, N. Fang, D. C. Vier, D. R. Smith, J. B. Pendry, D. N. Basov, and X. Zhang, Science **303**, 1494 (2004).
[4] S. Linden, C. Enkrich, M. Wegener, J. F. Zhou, T. Koschny, and C. M. Soukoulis, Science **306**, 1351 (2004).
[5] V. M. Shalaev, W. Cai, U. K. Chettiar, H.-K. Yuan, A. K. Sarychev, V. P. Drachev, and A. V. Kildishev, Opt. Lett. **30**, 3356 (2005).
[6] V. M. Shalaev, Nat. Photonics **1**, 41 (2007).
[7] C. M. Soukoulis, S. Linden, and M. Wegener, Science **315**, 47 (2007).
[8] G. Dolling, M. Wegener, C. M. Soukoulis, and S. Linden, Opt. Lett. **32**, 53 (2007).
[9] M. W. Klein, C. Enkrich, M. Wegener, and S. Linden, Science **313**, 502 (2006).
[10] M. W. Klein, M. Wegener, N. Feth, and S. Linden, Opt. Express **15**, 5238 (2007).
[11] A. A. Zharov, I. V. Shadrivov, and Y. S. Kivshar, Phys. Rev. Lett. **91**, 037401 (2003).
[12] S. O'Brien, D. McPeake, S. A. Ramakrishna, and J. B. Pendry, Phys. Rev. B **69**, 241101(R) (2004).
[13] A. K. Popov and V. M. Shalaev, Appl. Phys. B: Lasers Opt. **84**, 131 (2006).
[14] R. S. Bennink, Y.-K. Yoon, R. W. Boyd, and J. E. Sipe, Opt. Lett. **24**, 1416 (1999).
[15] J. P. Huang, L. Dong, and K. W. Yu, J. Appl. Phys. **99**, 053503 (2006).
[16] S. Zhang, W. Fan, N. C. Panoiu, K. J. Malloy, R. M. Osgood, and S. R. Brueck, Opt. Express **13**, 4922 (2005).
[17] S. Zhang, W. Fan, N. C. Panoiu, K. J. Malloy, R. M. Osgood, and S. R. J. Brueck, Phys. Rev. Lett. **95**, 137404 (2005).
[18] W. Wu, E. M. Kim, E. Ponizovskaya, Y. Liu, Z. Yu, N. Fang, Y. R. Shen, A. M. Bratkovsky, W. Tong, X. Zhang, S.-Y. Wang, and R. S. Williams, Appl. Phys. A: Mater. Sci. Process. **87**, 143 (2007).
[19] W. Wu, Y. Liu, E. M. Kim, Z. Yu, N. Fang, X. Zhang, Y. R. Shen, and S. Y. Wang, Appl. Phys. Lett. **90**, 063107 (2007).
[20] See, for example, Y. R. Shen, *The Principles of Nonlinear Optics* (Wiley, New York, 1984), Chap. 2.
[21] For the SS case with incident plane along the broad Ag wire, for example, it can be seen that the resonant field distribution emphasizes the field at the edges of the wires where the symmetry breaking occurs but the nonresonant field distribution does not.